Internal Gravity Waves Generated by a Local Thermal Source in an Irrotational Zonal–Vertical Plane: Numerical Analysis①

Zhang Daizhou (张代洲)
Center for Environmental Sciences, Peking University, Beijing 100871
Tanaka Hiroshi (田中浩)
Institute for Hydrospheric–Atmospheric Sciences, Nagoya 464–01, Japan
Qin Yu (秦 瑜)
Geophysics Department, Peking University, Beijing 100871
Received May 3, 1995; revised August 11, 1995

ABSTRACT

The vertical and horizontal propagation of internal gravity waves forced by a local thermal source at the lower boundary is examined using the irrotational two–dimensional model developed by Zhang et al. (1995). The source generates waves with the same absolute frequency $1/15\ d^{-1}$ but different wavenumber. Internal gravity waves with wide spreading frequencies and wavenumbers appear due to wave–wave interactions. The forced waves 1W (westward–propagating with wavenumber 1) and 1E (eastward–propagating with wavenumber 1), whose absolute phase speeds are 31 m s^{-1}, are predominant. Other forced waves with smaller phase speeds are relatively weaker. These waves interact with the zonal mean flow, causing the flow to alternate with easterly and westerly with a 32–month period. The absolute maximum wind speeds of easterly and westerly are 35 m s^{-1} which is larger than the largest phase speed of forced waves. The forced waves 1E and 1W may accelerate easterly and westerly up to $\pm$ 31 m s^{-1}, respectively. The excessive accelerations are due to the self–acceleration of waves 1E and 1W or newly generated high frequency waves 1E and 1W.

The horizontal propagation of the waves are mainly affected by the forcing and wave–flow interactions which lead to fast–slow variations of wave phase speed and amplitude.

Key words: QBO, Wave–flow interaction, Wave–wave interaction, Wave self–acceleration

I. INTRODUCTION

On the basis of wave–flow interaction theory, many numerical models have been developed to study the long period oscillations (QBO) of zonal mean flow occurring in the lower equatorial stratosphere. The key factors in the theory are the two equatorial waves, Kelvin wave and mixed Rossby–gravity wave, and their interaction with zonal mean flow (Holton and Lindzen, 1972). However, most of the previous numerical models have only focused on the characteristics of the two waves by use of WKB approximation to estimate the mean flow acceleration and wave phase speeds (Plumb, 1977; Plumb and Bell, 1982; Dunkerton, 1981a, 1981b, 1985; Tanaka and Yoshizawa, 1985, 1987) or the assumption that the two waves were steadily excited at the bottom boundary (Takahashi, 1987; Takahashi and Boville, 1992).

In fact, most of the waves found in the equatorial stratosphere must be generated by local sources because steady global–scale sources have not been found so far in the tropical

①This study is partly supported by Chinese postdoctoral foundation.

stratosphere and troposphere. The tropopause temperature over Indonesia shows an approximately 15–20 day periodical variation (Tsuda et al., 1993) and the possibility that QBO is induced by local thermal activities has been proved by Zhang et al. (1995). Simulations with WKB assumption proposed that waves would be self–accelerated during their vertical propagation if they interacted with zonal mean flow (Tanaka and Yoshizawa, 1987). But there is no elucidation of such features when WKB approximation is not included.

In the present study, time–longitude Fourier transform is applied to analyze the deviations of zonal wind in order to clarify the behaviors of internal gravity waves during QBO's generation. The numerical model, including boundary and initial conditions, is the same as that described by Zhang et al. (1995). And the simulation case with 15K forcing amplitude, 5000 km forcing scale and 15 d forcing period is employed.

II. FEATURES OF ZONAL MEAN FLOW

The simulation is carried out for 2160 days. Fig. 1 shows the time–height cross section of 15–d averaged zonal mean flow after 360–d adjustment calculation. The main feature is that easterly and westerly wind regimes alternate regularly with a constant steady period of about 960 d (32 months). The successive regimes first appear from top boundary and descend at a rate of 1 km per month. The absolute maximum of wind speeds, 35 m s^{-1}, appears at 24 km whatever in easterly and westerly. These features are similar to QBO occurring in the lower equatorial stratosphere. From the analysis of wave source, the forced waves 1W and 1E have the largest phase speeds and the absolute values are 31 m s^{-1} (Zhang et al. 1995). Therefore, the maximum of zonal mean flow is 4 m s^{-1} larger than the largest phase speed of forced waves. Such features suggest that waves with larger phase speeds appear (Dunkerton, 1981a).

III. WAVE PROPERTIES

Applying Fourier transform, it is found that the forcing generates only the waves with frequencies of $-1/15$ d^{-1} and $1/15$ d^{-1} and the forced waves with the same wavenumbers propagate eastward and westward symmetrically. The power of the forced waves, line C shown in Fig. 2 of Zhang et al. (1995), indicated that longer waves with wavenumbers smaller than 4 dominated wave properties. But the latter seems to be much more complicated than that described by WKB theory during the generation of easterly and westerly. In this section, we detect the properties of waves 1W, 2W, 1E and 2E. Because the forcing is symmetric to the forcing center and the patterns of easterly and westerly regimes of the zonal mean flow are almost the same (Fig. 1), we examine the wave properties only during the period from day 630 to day 720 when the zonal mean flow is dominated by easterly. The wave properties during

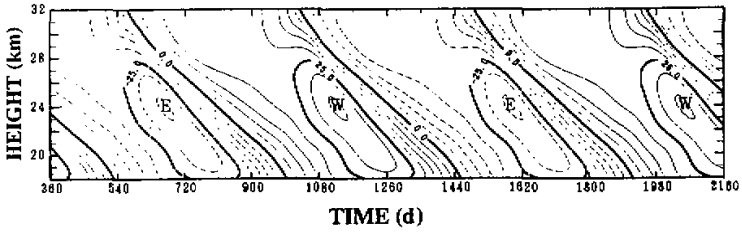

Fig. 1. Time–height cross section of 15–d averaged zonal mean flow after 360–d adjustment calculation. Contour intervals are 5 m s^{-1}. Regimes of westerly (W) and easterly (E) are drawn by thin solid curves and dashed curves, respectively.

the opposite episode when the zonal mean flow is dominated by westerly can be imagined upon the features from day 630 to day 720. The analysis data are sampled once a day. The 1-d time increment of the data results in a Nyquist frequency of 0.5 d^{-1} which is precise enough to determine the wave features in the present study.

1. *Power Spectrum Analysis*

Here, the wave properties are examined through frequency–wavenumber power spectra of the internal gravity waves. The power spectra are calculated at four levels of 18, 22, 26 and 30 km, respectively, and shown in Fig. 2.

The power spectra at 18 km show that waves with forcing frequency are predominant. Both eastward– and westward–propagating waves, even the waves with large wavenumbers, are active and approximately symmetrical. New waves with their frequencies rather than $1/15$ or $-1/15$ d^{-1} appear at this level, proving that wave–wave interactions occur. With the vertical propagation, westward–propagating waves are severely damped, which can be found from the spectra at 22 km. Almost all the westward–propagating waves disappear at 22 km except for wave 1W, suggesting that the critical levels for these waves exist between 18 and 22 km. The eastward–propagating waves do not have obvious variations below 26 km. Force waves propagate through the easterly regime and generate new waves. However, they are damped rapidly due to flow absorption after entering into the westerly regime.

It must be noted that newly generated high frequency waves with wavenumber 1 are found in both propagating directions at all levels. These waves pass through easterly or westerly regime because of their large phase speeds and probably contribute to the acceleration of zonal mean flow at middle levels.

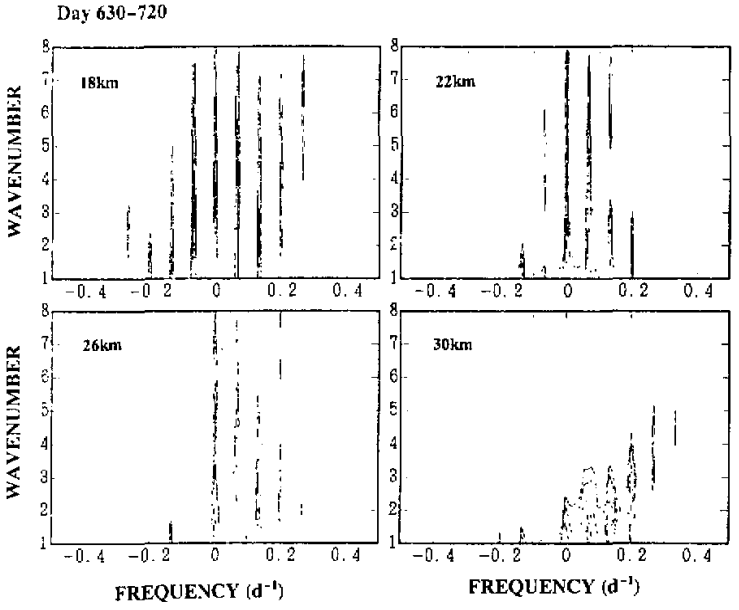

Fig. 2. Frequency–wavenumber power spectra of the zonal wind deviations for the time period from day 630 to day 720. Contours are spaced logarithmically from 0.01 to 10 with four contours per dekad.

2. *Zonal Wind Perturbation*

A great deal of information about wave behaviors are obtained by analyzing the zonal wind deviations caused by individual waves. Fig. 3 shows zonal–vertical cross sections of the components of waves 1W, 1E and 2E on day 675, when the zonal mean flow is easterly below 28 km and westerly above 28 km, and the maximum wind velocity of easterly is -35 m s^{-1} at 24 km (Fig. 1).

The component of wave 1W is considerably trapped below 20 km but its amplitude increases slightly being accompanied by the expansion of vertical wavelength between 20 and 24 km. Its critical level is at 28 km, above which its residual part propagates up to the top level. The damping of the waves suggests that wave–flow interactions occur. But the behaviors of wave 1W near 24 km seem to conflict with the wave–flow interaction theory that westward-propagating waves should be damped in easterly regime (Holton and Lindzen, 1972). In fact, between 22 and 26 km as shown in Fig. 2, the component of wave 1W forced by the source is weaker than that caused by newly generated wave 1W with the phase speed about -62 m s^{-1}. Because the maximum of easterly -35 m s^{-1}, the newly generated wave 1W is not effectively damped by zonal mean flow. In other words, the component of wave 1W near 24 km is probably dominated by the newly generated wave 1W of higher frequencies.

Wave 2W is originally weak and damped severely below 20 km because of its small phase speed. Its critical level appears at 21.5 km. On the contrary, waves 1E and 2E easily pass through the easterly regime propagating upward, accompanied by amplitude growth. As they approach to the transition level of zonal mean flow from easterly to westerly, their amplitudes increase and vertical wavelengths decrease rapidly. After they enter into the westerly regime, their amplitudes decrease rapidly due to the absorption of zonal mean flow.

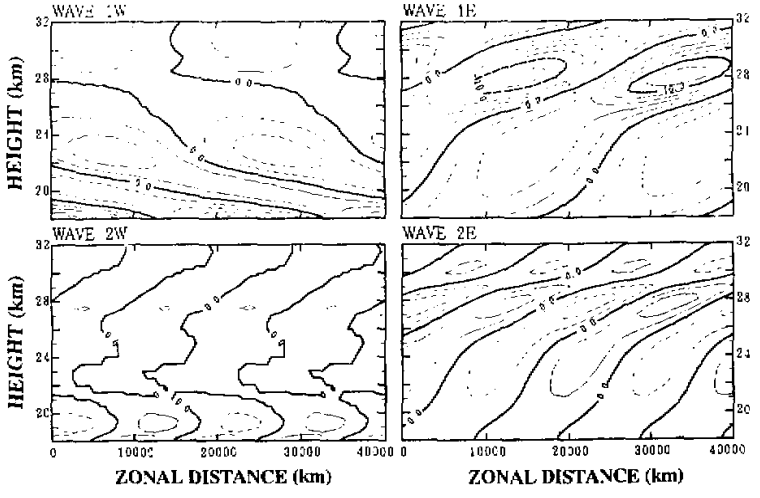

Fig. 3. Zonal–vertical cross sections of the zonal wind deviations from zonal mean wind cause by waves 1W, 2W, 1E and 2E on day 675. Positive values are drawn by thin solid curves and negative values are drawn by dashed curves. Contour intervals are 1 m s^{-1} for waves 1W and 2W and 2 m s^{-1} for waves 1E and 2E.

3. *Phase Speed, Amplitude and Group Velocity*

In order to detect precisely the vertical propagation features, the phase speeds amplitudes and group velocities of waves 1E, 2E, 1W and 2W are calculated using the method suggested by Takahashi (1987). Fig. 4 shows the vertical profiles of the phase speeds and amplitudes of the four waves on day 675 together with the vertical distribution of the zonal mean flow. It is assumed that the wave disappears if its apmlitude is smaller than 0.1 m s^{-1}.

The two eastward waves 1E and 2E, do not change very much under 25 km. Above 25 km they are accelerated, especially in the westerly regime. However, waves 1W and 2W interact with the zonal mean flow mainly in the easterly regime, leading to the acceleration of themselves. Between 20 and 24 km, the phase speed of wave 1W, averaged −60 m s^{-1}, is considerably different from its initial values of −31 m s^{-1}. Wave 2W is completely trapped below 21 km. Therefore, the maximum wind speed of easterly, −35 m s^{-1}, must be due to the appearance of wave 1W with larger phase speed. Unfortunately, it is impossible to divide wave 1W into self–accelerated part and newly generated part. Nevertheless, it is reasonable to conclude that the maximum wind velocities of easterly are determined by wave 1W and the values of −35 m s^{-1} are due to the larger phase speeds of the self–accelerated or newly generated wave

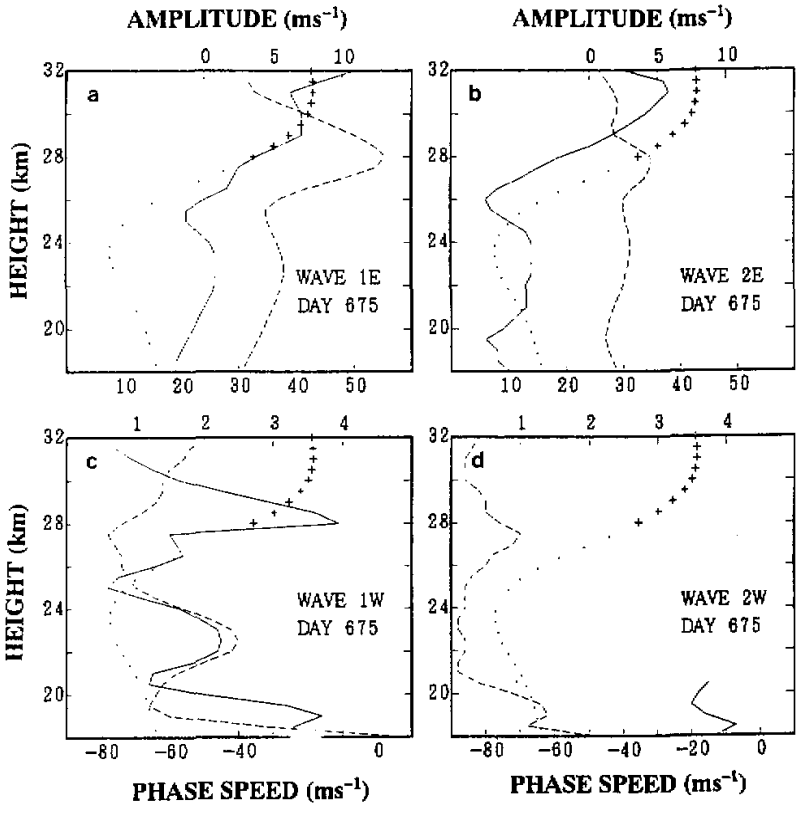

Fig. 4. Vertical profiles of the phase speeds (thin solid curves), and amplitudes (dashed curves) of waves 1E(a), 2E(b), 1W(c) and 2W(d) on day 675. The zonal mean flow on the day is illustrated in the four panels by dots (westeard) and cross (eastward) with the scale from −50 to 50 m s^{-1}.

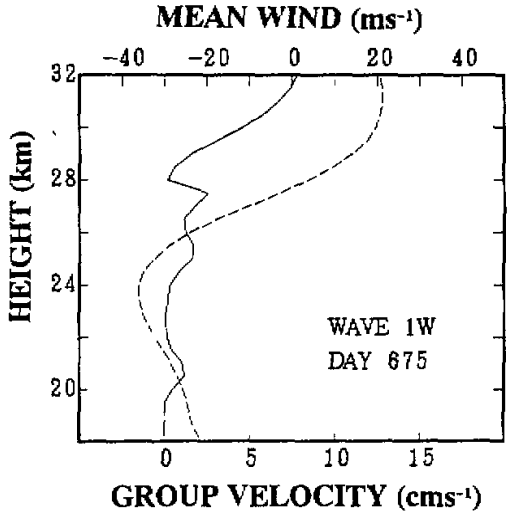

Fig. 5. Vertical profiles of the group velocity of wave 1W (thin solid curve) and the zonal mean flow on day 675 (dashed curve).

1W. Further evidence is given by the vertical profile of the group velocity of wave 1W on day 675, shown in Fig. 5 together with the zonal mean flow. Small group velocity corresponds to the strong easterly. Similarly, the self-accelerated or newly generated wave 1E is the reason why the maximum wind velocity of westerly is 35 m s^{-1}.

4. *Horizonal Propagation*

The horizontal propagation features are examined at 18 km level where the four waves are strong enough to be calculated. Time variations of the phase, phase speed and amplitude of waves 1W and 2W from day 660 to day 750 are shown in Fig. 6. The reference point of Fourier transform is chosen at the center of the forcing.

The variation of the phase speed indicates that wave 1W is accelerated or decelerated around −30 m s^{-1} with a period of 15 d during its horizontal propagation. Its amplitude also has a 15-d period variation. The variations of phase speed, amplitude and phase of wave 2W at 18 km are different from wave 1W. Wave 2W has a noticeable second amplitude peak every 15 days, proving that the horizontal propagation is affected by wave-flow interactions. Its phase speed oscillation has two main peaks and a third peak every 15 days, represented by 1, 2 and 3 in the figure, respectively. Peak 1 is likely to be associated with the forcing because it coincides with the positive amplitude increase of the forcing. Peak 2 seems to be controlled by wave-flow interaction because it is inversely proportional to the second peak of the amplitude. Peak 3 might be the residual part of the wave which has propagated more than one circle of the domain. Direct evidence can be got by comparing the behaviors of wave 2W with wave 2E which does not have peak 2 during this period (figure omitted).

IV.DISCUSSION

As reported above, because of wave-wave interactions, new waves with different frequencies from the forced waves appear. These waves interact with zonal flow, causing it to oscillate like QBO and the waves are accelerated through the interaction.

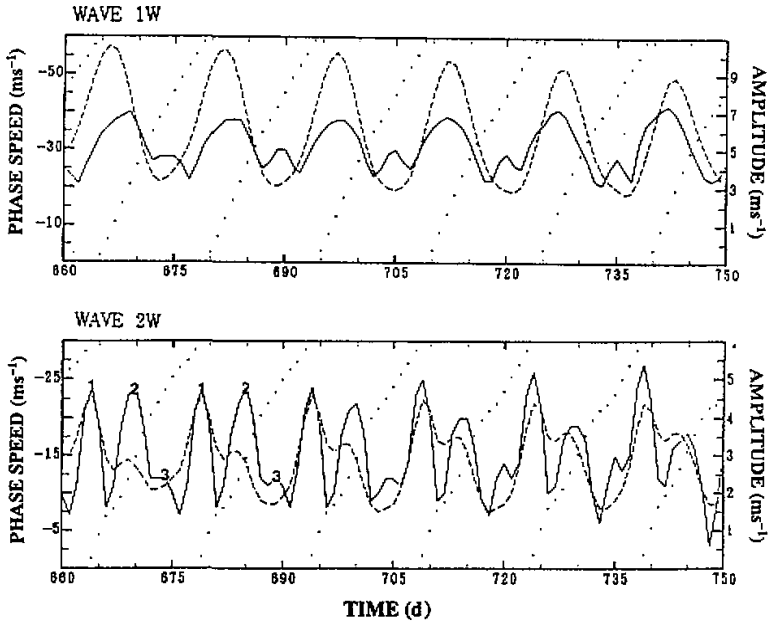

Fig. 6. Time variation of phase speeds (thin solid curves), amplitudes (dashed curves) and phase (dots, representing the phase change from 0 to 2π) of waves 1W and 2W at 18 km from day 660 to day 750.

1. *Wave–wave Interaction*

If there are two waves which are $\sin(k_1 x - \omega_1 t)$ and $\sin(k_2 x - \omega_2 t)$, their interaction means (Craik, 1984),

$$\sin(k_1 x - \omega_1 t)\sin(k_2 x - \omega_2 t). \tag{1}$$

As a result, this interaction generates two new waves:

$$\cos[(k_1 + k_2)x - (\omega_1 + \omega_2)t] \tag{2}$$

and

$$\cos[(k_1 - k_2)x - (\omega_1 - \omega_2)t]. \tag{3}$$

If the two interacting waves have different amplitudes, the two newly generated waves have different phases in (2) and (3) but the same wavenumbers and frequencies. The two new waves (2) and (3), once formed, will interact with each other and the pre–existing waves. From the analysis of Zhang et al. (1995), initially there are no other waves besides the forced waves which have the same frequencies and different wavenumbers. Therefore, the frequencies and wavenumbers of newly generated waves must be the sum or subtraction of the forced waves. It is impossible to divide the forced waves and newly generated waves in terms of wavenumber. Because the forcing has an unique frequency, $1/15\ \mathrm{d}^{-1}$, the newly generated waves must have the frequencies which are integer times of the forcing frequency. Fig. 2 shows clearly that the frequencies of the newly generated waves are $\pm n/15\ \mathrm{d}^{-1}(n=0,1,2,3,4,\cdots)$.

2. *Wave–self Acceleration*

Based on wave dynamics under a slowly varying assumption, the phase velocity obeys the following equation (Tanaka and Yoshizawa, 1985):

$$\frac{\partial c}{\partial t} + W_g \frac{\partial c}{\partial z} = \frac{\partial \bar{u}}{\partial t}, \tag{4}$$

where c is the phase velocity, W_g is the vertical component of the group velocity, $\bar{u}$ is the zonal mean flow, and the horizontal wavenumber k is assumed to be constant. Therefore, wave–self acceleration has close relations with the variation of zonal mean flow and should be never ignored as a basic mechanical process in wave–flow interaction. As reported by Tanaka and Yoshizawa (1985), due to such acceleration, easterly wind speeds would exceed the initial values of westward–propagating wave phase velocity and westerly wind speeds would exceed the initial values of eastward–propagating wave phase velocity, which is consistent with the present simulation results. The forced waves 1W and 1E have the largest phase velocities and the absolute values are 31 m s^{-1} but the absolute maximum wind speeds of zonal mean flow are 35 m s^{-1}.

In Fig. 4, there is another phenomenon. Waves 1E and 2E are considerably accelerated between 25 km and 28 km where is easterly region, which is inconsistent with WKB theory. It seems that such vertical distributions of the phase velocities are related to the decrease of zonal mean flow because the accelerations of waves 1E and 2E occur mainly in the easterly–to–westerly transition region. When $\bar{u}$ approaches the phase speed c, the vertical component of group velocity can be demonstrated by (Dunkerton, 1981a)

$$W_g = \frac{k}{N}(c - \bar{u})^2, \tag{5}$$

where N is the buoyancy frequency. Substituting (5) into (4), we get

$$\frac{\partial c}{\partial z} = \frac{N}{k}\frac{\partial}{\partial t}\left(\frac{1}{c - \bar{u}}\right). \tag{6}$$

Above 25 km, easterly flow rapidly decreases, which leads to

$$c - \bar{u} \rightarrow +0 \tag{7}$$

for eastward–propagating waves. Therefore, phase velocities of eastward–propagating waves begin to increase with height above 25 km, even in the easterly region.

V. SUMMARY

The two–dimensional model successfully reproduces the long period oscillation of zonal mean flow as expected by WKB theory. However, the present studies reveal that the wave properties are much more complicated than that described by WKB theory. The maximum of zonal mean wind velocity is 35 m s^{-1}, larger than the largest phase speed of the forced waves, 31 m s^{-1}.

Wave analysis shows that the internal gravity waves interact with not only zonal mean flow but also themselves to produce a great deal of new waves. Wave–flow interactions lead to wave self–acceleration. The forced waves 1E and 1W may accelerate westerly and easterly to $\pm$ 31 m s^{-1}, respectively. The self–accelerated or newly generated waves 1E and 1W further accelerate the zonal mean flow up to $\pm$ 35 m s^{-1}. Roles of other waves can be omitted.

The internal gravity waves propagate horizontally with oscillations of phase speed and amplitude. It is convinced that such oscillations are mainly affected by wave–flow interactions and the wave source. But the mechanism is still unclear.

Many results reported here have never been mentioned by previous works. The wave properties and their mechanisms cannot be demonstrated simply by WKB theory. It is not sure that the nonlinear wave–wave interactions and wave self–accelerations would occur in the real equatorial stratosphere. However, if the internal gravity waves are important for QBO, the present results prove that roles of wave–wave interactions and wave self–accelerations cannot be omitted in either theoretical or numerical studies.

REFERENCES

Craik, A.D.D. (1984), *Wave Interactions and Fluid Flows*, Cambridge University Press, pp. 322.

Dunkerton, T.J. (1981a), Wave transience in a compressible atmosphere, Part I: Transient internal waves, mean–flow interaction, *J. Atmos. Sci.*, **38:** 281–297.

Dunkerton, T.J. (1981b), Wave transience in a compressible atmosphere, Part II: Transient equatorial waves in the quasi–biennial oscillation, *J. Atmos. Sci.*, **38:** 298–307.

Dunkerton, T.J. (1985), A two–dimensional model of the quasi–biennial oscillation, *J. Atmos. Sci.*, **42:** 1151–1160.

Holton, J. R. and R.S. Lindzen (1972), An update theory for the quasi–biennial cycle of the tropical stratosphere, *J. Atmos. Sci.*, **29:** 1076–1080.

Plumb, R.A. (1977), The interaction of two waves with the mean flow: Implications for the theory of the quasi–biennial oscillation, *J. Atmos. Sci.*, **34:** 1847–1858.

Plumb, R.A. and R.C. Bell (1982), A model of the quasi–biennial oscillation on an equatorial beta plane, *Quart. J. Roy. Meteor. Sci.*, **108:** 335–352.

Takahashi, M. (1987), A two–dimensional model of the quasi–biennial oscillation: Part I, *J. Meteor. Soc. Japan*, **65:** 523–536.

Takahashi, M. and B.A. Boville (1992), A three–dimensional simulation of the equatorial quasi–biennial oscillation, *J. Atmos. Sci.*, **49:** 1020–1035.

Tanaka, H. and T. Yoshizawa (1985), QBO and its analog under the assumption of wave self–acceleration, *J. Atmos. Sci.*, **42:** 2350–2359.

Tanaka, H. and T. Yoshizawa (1987), A slow varying model of the quasi–biennial oscillation involving effects of transience, self–acceleration and saturation of equatorial waves, *J. Atmos. Sci.*, **44:** 1427–1436.

Tsuda, T. (1993), Radiosonde observation in Indonesia, *Proceedings of the Autumn Conference of Japanese Meteorological Society in 1993*, p. 19.

Zhang, D., Y. Qin and H. Tanaka (1995), QBO–like oscillations induced by local thermal forcing, *Adv. Atmos. Sci.*, **12:** 245–254.